Pamukkale Üniversitesi Mühendislik Bilimleri Dergisi
Pamukkale University Journal of Engineering Sciences

Numerical investigation of wind resistance and heat island formation in buildings of different configurations

Farklı konfigürasyonlardaki binalarda rüzgâr direnci ve ısı adası oluşumunun sayısal incelenmesi

Ömer Faruk CAN[1*]

[1]Department of Mechanical Engineering, Dicle University, Diyarbakir, Turkey.
faruk.can@dicle.edu.tr

Received/Geliş Tarihi: 27.07.2023 Revision/Düzeltme Tarihi: 18.12.2023 doi: 10.5505/pajes.2023.51813
Accepted/Kabul Tarihi: 20.12.2023 Research Article/Araştırma Makalesi

Abstract

As a result of increasing population density, problems in residential areas have emerged in cities in recent years. With the development of technology, engineers have turned to the construction of taller buildings to meet the increasing demand. As a result, heat island formation becomes inevitable if there is not enough distance between buildings. In this study, it is aimed to numerically investigate the heat island formation and wind effects in buildings. The Ansys Cfx software program was used for the modeling process. Six different building configurations were analyzed to investigate heat island formation. Building heights and inter-building distances were varied for different aspect ratios. As a result of the study, more heat islands formed when the distance between buildings was smaller. As a result of the study, more heat island formation was observed in the first four cases (C1--C4). C5 and C6 were found to be the most suitable building sequences. drag coefficients (Cd) were obtained in the range of 1.35 to 1.65 for different building sequences. As a result of the cooling effects of the wind on the building, a decrease of 2 to 5 degrees in the average temperature of the building was observed. The average heat transfer coefficient is (68 W/mK) when only concrete is used in buildings. The best insulation was realized when glass wool was used.

Keywords: Heat island, numerical modeling, wind effect, urban planning, insulation material

Öz

Artan nüfus yoğunluğunun bir sonucu olarak, son yıllarda şehirlerde yerleşim alanlarında sorunlar ortaya çıkmıştır. Teknolojinin gelişmesiyle birlikte mühendisler artan talebi karşılamak için daha yüksek binaların yapımına yönelmişlerdir. Sonuç olarak, binalar arasında yeterli mesafe olmadığı takdirde ısı adası oluşumu kaçınılmaz hale gelmektedir. Bu çalışmada binalarda ısı adası oluşumu ve rüzgar etkilerinin sayısal olarak incelenmesi amaçlanmıştır. Modelleme işlemi için Ansys Cfx yazılım programı kullanılmıştır. Isı adası oluşumunu incelemek için altı farklı bina konfigürasyonu analiz edilmiştir. Bina yükseklikleri ve binalar arası mesafeler farklı en-boy oranları için değiştirilmiştir. Çalışma sonucunda, binalar arasındaki mesafe azaldıkça daha fazla ısı adası oluştuğu görülmüştür. Çalışma sonucunda ilk dört durumda daha fazla ısı adası oluşumu gözlenmiştir(C1—C4). En uygun bina diziliminin C5 ve C6 olduğu görülmüştür. Sürüklenme katsayıları (Cd) farklı bina dizilimleri için 1.35 ile 1.65 aralığında elde edilmiştir. Rüzgarın bina üzerindeki soğutma etkileri sonucunda binanın ortalama sıcaklığında 2 ila 5 derecelik bir düşüş gözlemlenmiştir. Binalarda sadece beton kullanıldığında ortalama ısı transfer katsayısı (68 W/mK) olmaktadır. En iyi yalıtım cam yünü kullanıldığında gerçekleşmiştir

Anahtar Kelimeler: Isı adası, sayısal modelleme, rüzgar etkisi, kentsel planlama, yalıtım malzemesi

1 Introduction

Urban heat islands are a problem, especially in big cities. In areas consisting of high-rise buildings, it is inevitable that the temperature will increase, especially on the lower floors. With the increase in temperature in these areas, the air temperature, which is already high in the summer, can rise to undesirable levels. This temperature negatively affects life in the summer. In addition, undesirable situations such as noise and vibration occur on building surfaces due to the incoming wind hitting the buildings and changing directions. There are many studies on urban heat islands in the literature. Kotharkar et al. conducted a numerical study on urban heat islands [1]. In their study, they investigated the heat island in terms of physical and geometrical aspects. A similar study [2] was carried out by Liu et al. and focused on groundwater temperatures in summer months with a numerical approach. Wang et al. [3] investigated the weak wind effects of urban heat islands.

The three physical elements of a city that have an impact on outdoor air temperature and urban heat island (UHI) intensity are buildings, pavements, and vegetation [4]. In specifically, the thermal properties of those three physical components—heat absorption from solar radiation during the day and heat release to the air during the night—depend on the heat island intensity (HII) [5]. The material's thermophysical qualities, such as density, thermal conductivity, and specific heat, influence how it absorbs and releases heat [4]. The UHI intensity is also influenced by the local weather, seasonal patterns, and environmental circumstances during the day and night [4,5]. There are reports on the thermal behavior of building exterior materials in walls [6,7], roofs [8,] and pavements [9]. According to reports on the thermal behavior of building exterior materials for walls [6,7], roofs [8,] and pavements [9], have a sizable impact on the duration and intensity of UHI in the corresponding area. In addition to vegetation [11] and transportation [12], other potential factors that may affect the urban climate include the thermal behavior of structures [10].

Reviews of the literature have reviewed numerous research examining the energy efficiency of urban buildings. For instance, Jige and Li examined the relationship between urban

*Corresponding author/Yazışılan Yazar

design and buildings' energy efficiency in a number of research, coming to the conclusion that these analyses had discovered a significant connection where urban form effects energy usage by between 100% and more than 400% [13]. The same authors also examined urban density and construction typologies, concluding that there is no clear correlation between urban building density and energy consumption and emphasizing the widely held belief that single-family homes use more energy than multifamily homes [13]. However, there hasn't been much discussion of the quantitative and qualitative examination of the relationship between the UHI and the energy performance of the buildings in other literature studies. In this regard, Santamouris' review is noteworthy since the author compared the energy efficiency of urban and rural structures, which resulted in an average increase in cooling demand of 23% and a corresponding average decrease in heating of 19% as a result of UHI [14.] Santamouris, 2014. Similar to this, Li et al.'s review found that the relationship between UHI and energy use led to an average 19% rise in cooling and a 16% decrease in heating 18.7% of the 24 case studies examined [15, 16]. There are many studies on urban heat islands [17-25].

In this study, using the ANSYS CFX software program, 3D models of buildings for 6 different cases were investigated. Building heights and distances between buildings were changed. As a result of these changes, heat island formation is analyzed. Temperature, streamlines, building insulation materials, drag coefficients, and wind speeds are considered. The cooling effects of the wind on the building and heat island formation are analyzed in line with these data. In previous studies, wind effects and heat island formation on parallel buildings of fixed height have been investigated. In this study, building heights and horizontal and vertical distances between buildings were changed. In this respect, it differs from other studies.

2 Material and Method

Using the ANSYS CFX software program, 3D models of the buildings were analyzed for six different cases. Analyses were performed for steady state. In all cases (C1—C6), a total of 20 buildings were modeled as 5x4 rows. In the first case (C1), the building heights were designed as 20, 40, 60, 80, and 100 m, and the wind direction was given from low to high. In the second case (C2), the building heights remained the same (from high to low), and the wind direction was the opposite of the first case. In the third case (C3), the building heights were chosen to be constant at 20 m. In the fourth case (C4), building heights are modeled as 100, 60, 20, 60, and 100, respectively. In the fifth (C5) and sixth cases (C6), building heights are modeled as being constant at 100 m. In the first four cases, the horizontal distance between buildings is 5 m and the vertical distance is 20 m. In the fifth case (C5), the horizontal distance between buildings is 20 m, and the vertical distance is 20 m In the sixth case (C6), the horizontal distance between buildings is 40 m, and the vertical distance is 40 m. The purpose of changing the building height and the distance between buildings is to study the effects of wind and heat island formation. Figure 1 shows the dimensions for the top view of the building and the horizontal column to be used for the building insulation materials in the first four cases. To study the effects of heat transfer in buildings in more detail, four different horizontal rows are considered. Horizontal row directions are given in figure 1. These horizontal cases are analyzed only for C1. The first row is covered with foam glass, the second row with cement coating, the third row with fireclay, and the fourth row with polyurethane foam. Isolation material thicknesses in buildings are taken as 4 cm. The thermophysical properties of insulation materials used in buildings are given in Table 1.

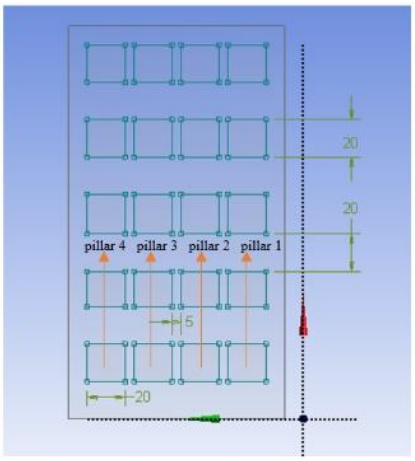

Figure 1. Dimensions in top view for C1-- C4

Table 1. Thermophysical properties of isolation materials used in buildings

İsolation material	ρ [kg/m³]	Cp [J/kg]	k [W/m°C]
Glass wool	60	1260	0.0385
Cement covering	1860	840	0.81
Firebrick	1120	790	0.9
Polyurethane Foam	30	1045	0.026

2.1 Mesh Development and Boundary Conditions

Figure 2 shows the general boundary conditions for all cases Wind speeds are taken at 40 m/s to better observe the possible effects. The air inlet temperature is 298 K, and the turbulence intensity is 5%. k-ε turbulence model is chosen. Building surfaces are at a constant temperature of 313 K. A wall boundary condition is given to the bottom surfaces. The other parts surrounding the buildings are given an open boundary condition (Topening = 298 K, Popening = 1 atm). Figure 3 shows the models and boundary conditions considered for six different cases. The flow direction is given from the left in all cases.

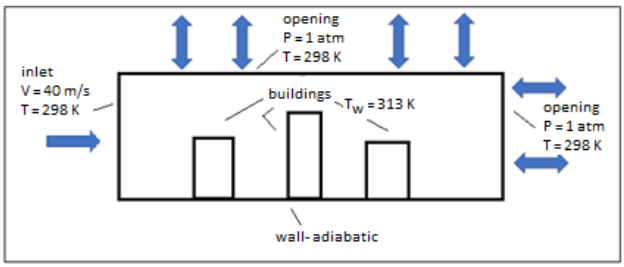

Figure 2. Boundary conditions (C1...C6)

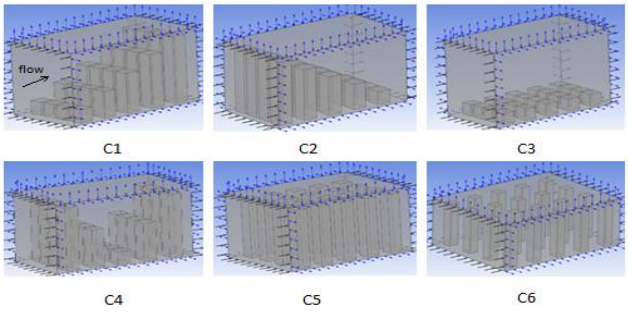

Figure 3. Models and flow directions (C1...C6)

In Table 2, grid independence analysis (C1) is given for different element numbers. The calculations are based on the average building interface temperatures. Deviations in these interface temperatures values were used for calculations using equation 1 (p. 386) [26]. As a result of the calculations, the most suitable network value was selected as value 2. The number of iterations was chosen as 1000. The convergence values in the momentum and energy equations were chosen to be equal to 1 x 10-7. Figures 5.a and 5.b show the detailed model and grid structure for C1. Figure 5.b shows the uniform mesh structure. Table 3 shows the number of elements, number of nodes, and skewness walues. It is desired that the skewness value be less than 1. For a good solution, it is preferred to be less than 0.5. Ideal values are 0.3 and below.

Table 2. Mesh independence analysis (C1) is given for different element numbers.

C1	Element numbers	Average building interface Temperatures [K]
Value 1	295684	304.86
Value 2	**331337**	**301.25**
Value 3	345236	301.65

$$\text{Convergence}_{12}\ \% = \left|\left(\frac{\text{value 1}-\text{value 2}}{\text{value 1}}\right)\right| 100 \qquad (1)$$

For verification of the study, first a comparison was made with a similar study. The wind distribution between parallel buildings was studied by B. Blocken et al.[27] The wind exposure of 40x20x20 parallel buildings was compared with this study. The distance between buildings was taken as 6 m. In the figure 4, the change of amplification factors ($K_{pcl} = u/u_0$) is given dimensionlessly. Looking at figure 4, it can be seen that the study is in harmony. The study is approximately 8–12% compatible with experimental results and 2–6% compatible with numerical results.

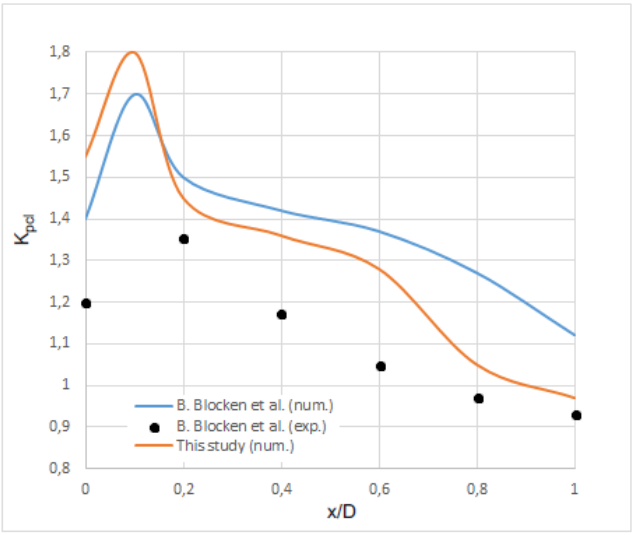

Figure 4. Compatibility of the study with the literature

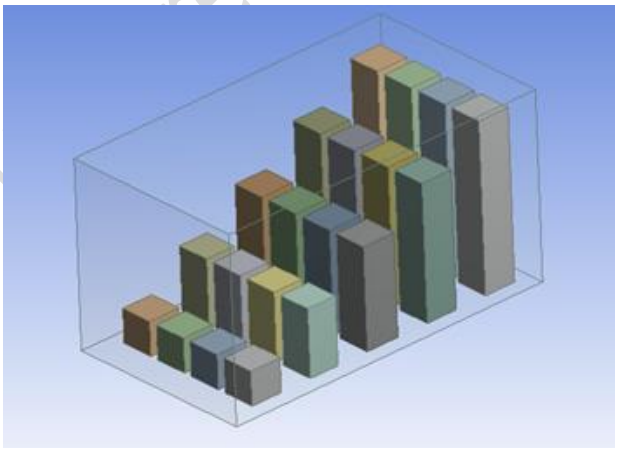

Figure 5.a). Model demonstration (C1)

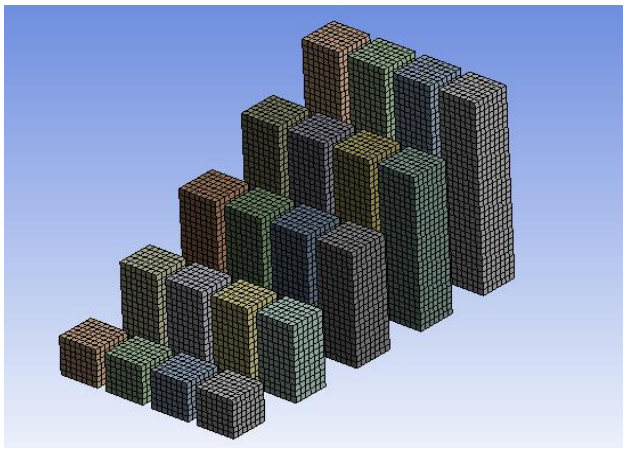

Figure 5.b. Mesh structure (C1)

Figure 5. Model and mesh structure

Table 3. Mesh details for all cases

Case	Element numbers	Node numbers	Skewness Values
C1	331337	6640	0.245
C2	331337	6640	0.245
C3	333858	6750	0.268
C4	334656	7232	0.362
C5	335015	7549	0.345
C6	330824	6579	0.268

2.2 Governing Equations

In this study, the k-ε turbulence model is used. k-ε turbulence model is the most widely used model. The full k-ε equations contain many unknown and unmeasurable terms. For a much more practical approach, the standard k-ε turbulence model is used, which is based on our best understanding of the processes involved, thus minimizing the unknowns, and providing a set of equations that can be applied to a large number of turbulent applications [28-33].

For turbulent kinetic energy k;

$$\frac{\partial(\rho k)}{\partial t}+\frac{\partial(\partial k u_i)}{\partial x_i}=\frac{\partial}{\partial x_j}\left[\frac{\mu_t}{\sigma_k}\frac{\partial k}{\partial x_j}\right]+2\mu_t E_{ij}E_{ij}-\rho\varepsilon \quad (2)$$

For dissipation

$$\frac{\partial(\rho\varepsilon)}{\partial t}+\frac{\partial(\partial\varepsilon u_i)}{\partial x_i}=\frac{\partial}{\partial x_j}\left[\frac{\mu_t}{\sigma_\varepsilon}\frac{\partial\varepsilon}{\partial x_j}\right]+C_{1\varepsilon}\frac{\varepsilon}{k}2\mu_t E_{ij}E_{ij}-C_{2\varepsilon}\rho\frac{\varepsilon^2}{k} \quad (3)$$

where, u_i term; represents velocity component in corresponding direction, E_{ij} term; represents component of rate of deformation and μ_t term; represents eddy viscosity.

$$\mu_t=\rho C_\mu\frac{k^2}{\varepsilon} \quad (4)$$

The equations also consist of some adjustable constants σ_k , σ_ε, $C_{1\varepsilon}$ and $C_{2\varepsilon}$. These are as follows

$C_\mu = 0.09$, $\sigma_k = 1.00$, $\sigma_\varepsilon = 1.30$, $C_{1\varepsilon} = 1.44$, $C_{2\varepsilon} = 1.92$

3 Results and Discussions

In this section, the temperature, velocity, and flow lines that appear in and around the buildings are examined. In addition, velocity and temperature changes are given graphically for each case. For this, two different planes are discussed. The horizontal plane is selected for the top view. To observe the effects of the heat island, plane 1 was chosen 10 m above the building floor (for all cases). The vertical plane was chosen for the side view. Here, the vertical middle of the buildings is chosen. (z = 55 m, C1). This is different for each model. Figure 6.a shows the selected vertical plane, and Figure 6.b shows the selected horizontal plane. The line chosen for the graph is 10 m above the ground and towards the back of the buildings. This is different for each model (for C1, x1 = 0, x2 = 125 m, y1 = 10 m, y2 = 10 m, z1 = 130 m, z2 = 130 m). Figure 7 shows the position of line 1 in the model.

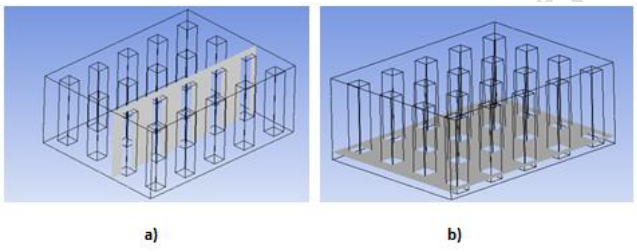

Figure 6. Horizontal and vertical planes selected for analysis results

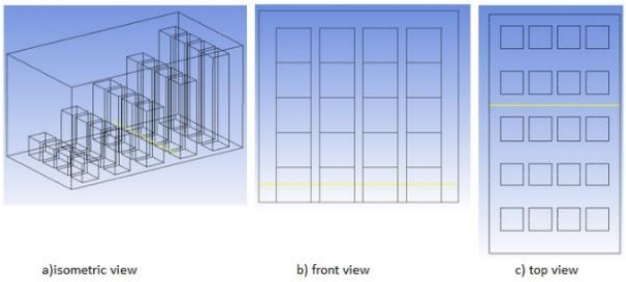

Figure 7. The location of the line 1 selected for the graphic results.

3.1 Heat transfer effects:

Figure 8. shows the temperature contours for plane 1 and six different cases. When the heat island formation results for plane 1 are analyzed, similar results are observed for the first four cases. Heat island formation was observed even if the building sequences changed. However, low temperatures are observed between buildings in C3 and C4. The main reason for heat island formation here is the distance between the buildings rather than the building arrangement. When C5 and C6 are analyzed, no heat island formation is observed when the distance between buildings is increased by 4 and 8 times, respectively, compared to the first four cases. Figure 9 shows the heat island formation for C1. Heat island formation is higher, especially near the bottom (red and orange regions).

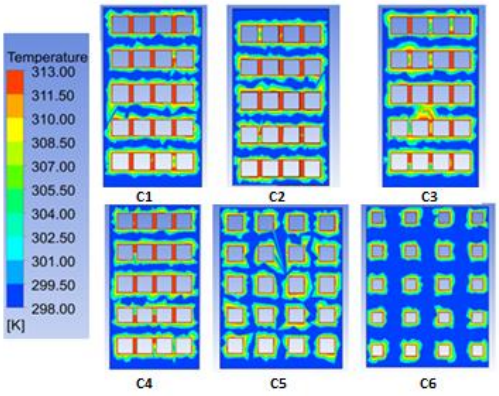

Figure 8. Temperature zones (plane 1)

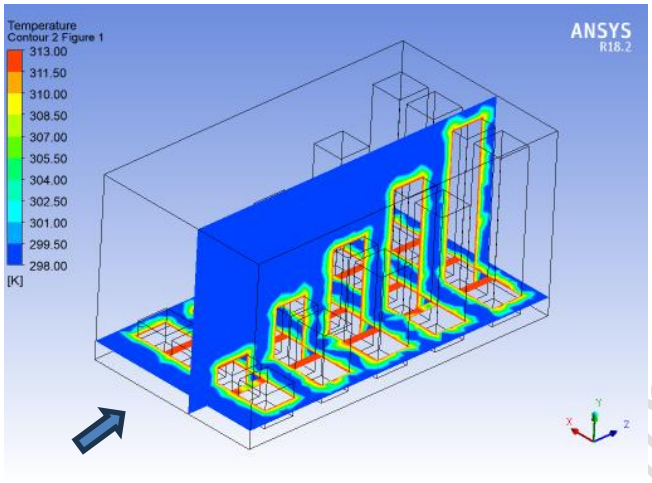

Figure 9. Temperature countour (plane 1, plane 2, C1)

On the temperature graphs obtained from line 1 in Figure 10, 100 points were chosen on the horizontal axis to obtain a precise result. The horizontal axis is shown as dimensionless (x/L). When the temperature graphs are examined, the temperature is high in the central regions of the model, as expected in cases 1, 2, 3, and 4. Especially in C 1, 2, and 4, the temperature values were higher than the other status averages in the middle regions. However, the highest temperature increases in the central region came out at 4. This situation was caused by the arrangement of the buildings.

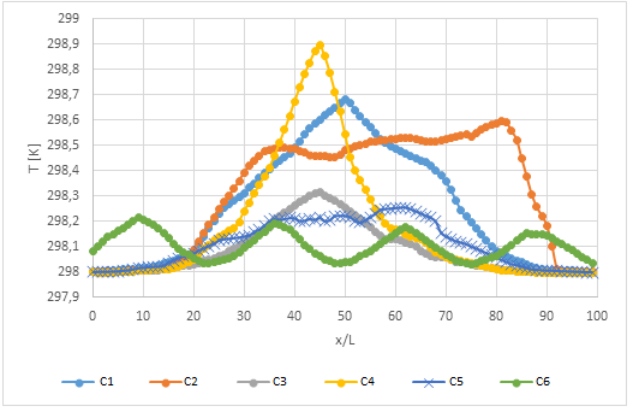

Figure 10. Temperature values (line 1)

The average heat transfer coefficients obtained when the building is covered with insulation materials are given in Table 4. When only concrete is used in buildings, the average heat transfer coefficient is 68. In the case of using only concrete, the heat loss is 17,64%. When glass wool is used, 4.38% of the heat is lost. The use of firebrick had an effect like that of concrete. Heat loss was realized at 16.65%. When polyurethane foam was used, only 1.15% heat loss occurred. Table 5 shows the average heat transfer coefficients, and average building temperatures number values obtained for six different cases (without insulation).

Table 4. Average heat transfer coefficients when the building is covered with insulation materials.

C1	**İsolation materials**	**Average heat transfer coefficient [W/m² K]**	**Building side and rear surface average temperatures [K]**	**Average Building interface temperatures [K]**
Pillar 1	Glass wool	59.79	310.88	301.51
Pillar 2	Cement covering	75.79	308.75	301.52
Pillar 3	Firebrick	74.88	308.87	301.52
Pillar 4	Polyurethane foam	61.70	310.36	301.51

Surjamanto et al. [34] obtained a temperature increase of 3.2 °C for firebrick and 2.6 °C for glass wool when using building insulation materials. However, the problem considered in this study is a cooling problem. The aim here is to ensure that the high wind speed cools the building as much as possible. In this study, a cooling of between 2 and 5 °C was realized with the use of different insulation materials. The lowest temperature drop of 4.25 °C was realized in the cement covering without insulation, and the highest temperature drop of 2.12 °C was realized in the use of glass wool. In a similar study, Meng et al. [35] reduced building average temperatures by about 2.1 C, Boccalatte et al. [36] by 2.75 °C, Gunawardena and Steemers [37] by 1.7 °C, and Guattari et al. [38] by 1.4 °C.

Table 5. Average heat transfer coefficients, average building temperatures (uninsulated)

Case	Average heat transfer coefficient [W/m² K]	Building average temperatures [K]
C1	68.03	298.21
C2	62.65	298.23
C3	90.43	298.22
C4	66.27	298.14
C5	70.08	298.10
C6	66.23	298.12

When Table 5 is examined, the lowest heat transfer was realized at C2. The highest heat transfer was realized at C3. Similar heat transfer values were observed at C 1,4,5 and 6. Figure 11.a shows the average wall heat transfer coefficient obtained from line 1 for six different cases. In the first 4 cases, the inter-building heat transfer is higher toward the back of the buildings according to the wind direction. In C5 and C6 the heat transfer is distributed towards the center of the building. For better observation, C5 and C6 are given separately in Figures 11.a and 11.b.

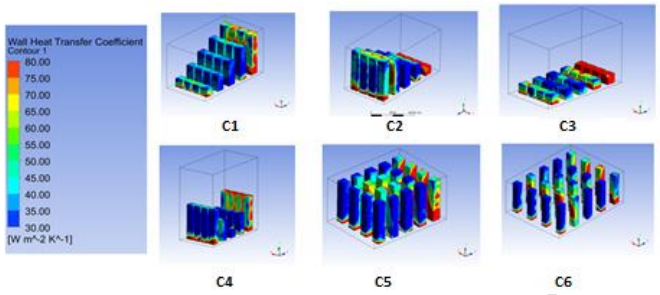

Figure 11.a. Average wall heat transfer coefficient values (C1—C6)

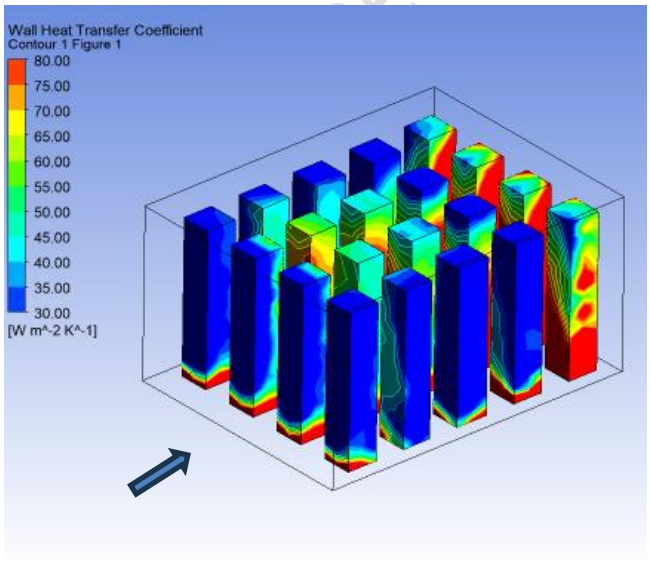

Fig 11. b. Average wall heat transfer coefficient values (C5)

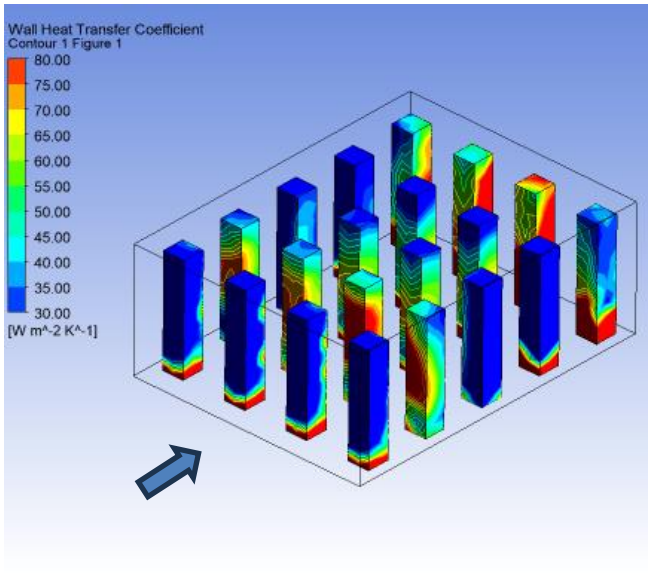

Figure 11.c. Average wall heat transfer coefficient values (C6)

3.2 Wind effects and velocity contour changes:

When the results of the velocity contours for the 1st plane are analyzed, it is determined that the wind is interrupted by the structures between the buildings in the first 4 cases. This situation shows that the wind changes direction rapidly. As a result of this situation, problems such as vibration and noise may occur in the buildings. In C5 and C6, it is found that the flow lines between the buildings are smoother. This is more suitable for vibration and noise.Figure 12.a and figure 12.b shows the velociy contour for C5 and C6, plane 1.

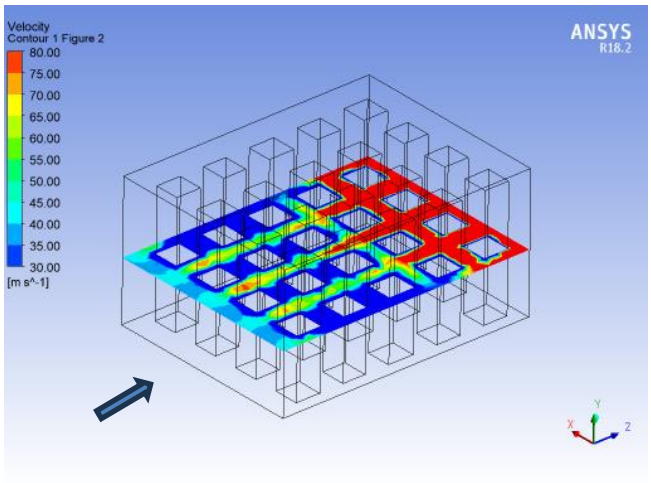

Figüre 12.a. Velocity contour (plane 1, C5)

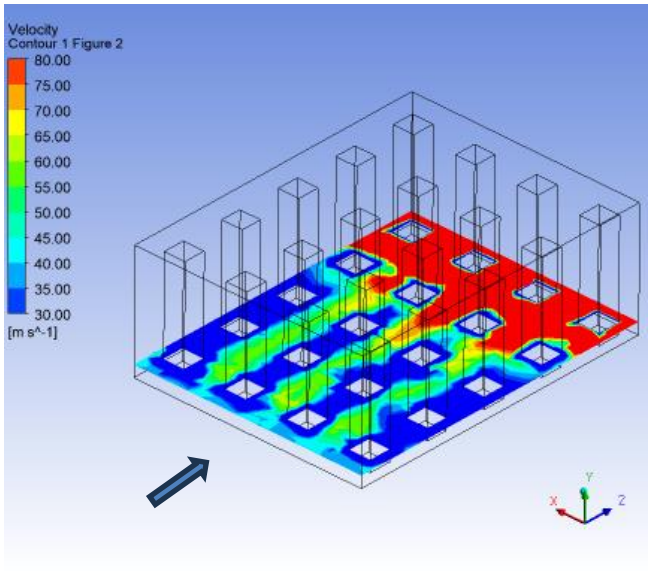

Figüre 12.b. Velocity contour (plane 1, C6)

Figure 13 shows the average wind speed values obtained from row 1 for six different cases. To obtain a precise result, 100 points were selected on the horizontal axis. When the velocity graphs are analyzed, while the situation in the selected regions C1, C2, and C4 is at average values, the situation in regions C3 and C5 is above the average values. Especially in C5 and C6, the speed is higher than expected. In this case, building arrangements are also effective.

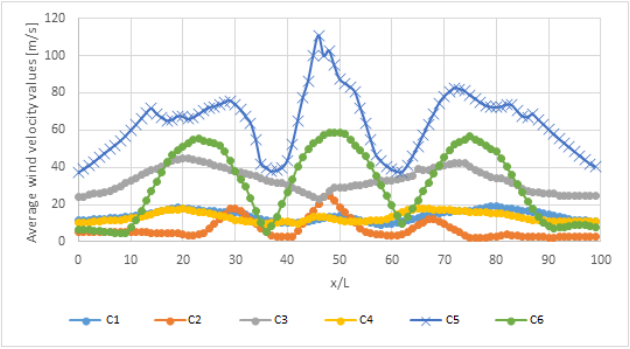

Figure 13. Average wind speed values (line 1)

3.3 Effect of drag coefficients around buildings:

The drag coefficient is an important parameter to observe the effects of wind resistance around the building. This value gives us an idea about the severity of the building's exposure to wind. Since the cross-sectional areas are square with a size of 20 m x 20 m, the hydraulic diameter is taken as 20 m. Inlet velocity is taken as 40 m/s. At 25 ^{o}C, the kinematic viscosity for air was taken as 15.89 x 10^{-6}. Re = 50.42x10^{6} was obtained for the study. In the case of Re 1, Cd = 24/Re. But for Re> 10^{4} and beyond, the resistance coefficients generally remain constant. In two-dimensional squares with sharp corners, Cd takes a value of about 2.2. In 3-dimensional high-rise buildings, Cd takes on a value of about 1.4 [39].

$$Cd = Fx/ [1/2\rho V^2 A] \quad (6)$$

Here ρ the term is air density, Fx term is force in horizontal direction, Cd term is drag coefficient, A term for this is frontal area.

Table 6. Consistency of drag coefficients around the building with the literature (ρair = 1.185 kg/m^3, B/D =1)

Case	C_d	% deviation		
		Ref. [39]	Ref. [40]	Ref. [41]
C1	1.35	3.70	18.51	22.22
C2	1.46	4.10	9.58	13.01
C3	1.32	6.06	21.21	25.12
C4	1.49	6.04	7.38	10.73
C5	1.45	3.44	10.34	10.79
C6	1.65	15.15	3.03	0.05

Similar studies have been carried out on the flow state over different geometries [42-44]. Using Equation 6, the values in Table 6 are obtained [38]. The agreement of the drag coefficients around the building with the literature is given in Table6. The lowest drag coefficient is obtained in case 1, and the highest in C6. This is since, as the building spacing increases, the wind continues its path without any breaks. This is an advantage in terms of the wind cooling the building and a disadvantage in terms of noise.

4 Conclusions

As a result of the study, more heat island formation was observed in the first four cases. The highest drag coefficient was observed in C6 (Cd = 1.65). The lowest average building surface temperatures were observed in C5 and C6. The average heat transfer coefficient is 68 when only concrete is used in the buildings. The heat loss is 17.64% when only concrete is used. When glass wool is used, 4.38% of the heat is lost. The use of firebricks had a similar effect to that of concrete. The heat loss was 16.65%. When polyurethane foam was used, only 1.15% of the heat was lost. It is observed that the heat transfer effects are higher in the center of the building compound. It is determined that the cooling effects of the wind on the building are between 2 and 5 degrees.

5 Author contribution statements

The author conducted the literature review, modeling and conclusion sections of the study.

6 Ethics committee approval and conflict of interest statement

There is no need to obtain permission from the ethics committee for the article prepared. There is no conflict of interest with any person / institution in the article prepared.

Nomenclature

A	Frontal area [m2]
C	Case
Cd	Drag coefficients [Fx / (1/2ρV2A)]
Cp	Specific heat capacity [J/kg]
F	Force [N]
Fx	x direction Force [N]
h	Heat transfer coefficient [W/m2K]
k	Heat conduction coefficient [W/mK]
Nu	Nusselt number [hD/k]
Pr	Prandtl number [Cpμ/k]
Re	Reynolds number [ρVD/μ]
T	Temperature [oC]
ρ	Denstiy [kg/m3]
V	Velocity [m/s]
ΔCP	Total surface pressure difference coefficient [-]
σk	Adjustable constants
σε	Adjustable constants
C1ε	Adjustable constants
C2ε	Adjustable constants
ui	Velocity component in corresponding direction,
Eij	Component of rate of deformation
μt	Eddy viscosity

7 References

[1] Rajashree K, Anurag B, Aparna R. "Assessing urban drivers of canopy layer urban heat island: A numerical modeling approach". *Landscape and Urban Planning*, 190, 103586, 2019.

[2] Chun L, Bin S, Chaosheng T, Lei G. "A numerical and field investigation of underground temperatures under Urban Heat Island". *Building and Environment*, 46, 1205-1210, 2011.

[3] Qun W, Yifan F, Jian H, Yuguo L. "Interacting urban heat island circulations as affected by weak background Wind". *Building and Environment*, 160, 106224, 2019.

[4] Phelan P.E, Kaloush K., Miner M., Golden J., Phelan B., Silva H., Taylor R.A., "Urban heat island: mechanisms, implications, and possible remedies". *Annual Review of Environmental Resources*, 40, 285–307, 2015.

[5] Tzavali A., Paravantis J.P., Mihalakakou G., Fotiadi A., Stigka E., "Urban heat island intensity: a literature review". *Fresenius Environmental Bulletin*, 24, (12), 4537, 2015.

[6] Jannat N., Hussien A., Abdullah B., Cotgrave A., "A comparative simulation study of the thermal performances of the building envelope wall materials in the tropics". *Sustainability*, 12, 4892, 2020.

[7] Larsen S.F., Filippín C., Lesino G., "Thermal behavior of building walls in summer: comparison of available analytical methods and experimental results for a case study". *Building Simulation,* 2, 3–18, 2009.

[8] Sahnoune S., Benhassine N., "Quantifying the impact of green-roofs on urban heat island mitigation", *International Journal of Environment and Sustainable Development*, 8, (2), 2017.

[9] Mohajerani A., Bakaric J., Bailey T. J., "The Urban Heat Island effect, its causes, and mitigation, with reference to the thermal properties of asphalt concrete", *Journal of Environmental Management*, 197, 522-538, 2017.

[10] Wonorahardjo S. "New concepts in districts planning, based on heat island investigation". *Procedia - Social and Behavioral Sciences*, 36, 235–242., 2012.

[11] Alves E.D.L., Lopes A.. "The urban heat island effect and the role of vegetation to address the negative impacts of local climate changes in a small Brazilian city". *Atmosphere*, 8, (2), 18, 2017.

[12] Louiza H., Z´eroual A., Djamel H.. "Impact of the transport on the urban heat island". *International Journal for Traffic and Transport Engineering*, 5, (3), 252–263., 2015.

[13] Jige, S., Li, C. "Urban form and building energy use : a systematic review of measures, mechanisms, and methodologies". *Renewable and Sustainable Energy Reviews*, 139, 110662, 2021.

[14] Santamouris, M. "On the energy impact of urban heat island and global warming on buildings". *Energy and Buildings*, https://doi.org/10.1016/j. enbuild.2014.07.022., 82, 100–113, 2014.

[15] Li X., Zhou, Y., Yu S., Jia G., Li H., Li W. "Urban heat island impacts on building energy consumption: a review of approaches and findings". *Energy*, 174, 407–419. https://doi.org/10.1016/j.energy.2019.02.183., 2019.

[16] Ref y Rafael E. L´opez G., Konstantin V., Guillermo A. Moncada-M., Manuel C. "How do urban heat islands affect the thermo-energy performance of buildings?". *Journal of Cleaner Production*, 373, 133713, 2022.

[17] Yukitaka O., Tomohiko I., Yukihiro K., Nanami S. "Numerical simulations of influence of heat island countermeasures on outdoor human heat stress in the 23 wards of Tokyo, Japan". *Energy and Buildings*, 114, 104–111, 2016

[18] Ilaria P., Marta C., Anna L. P., Gabriel P., Luisa F. C. "Inter-building assessment of urban heat island mitigation strategies: Field tests and numerical modelling in a simplified-geometry experimental set-up". *Renewable Energy*, 147, 1663-1675, 2020.

[19] Zhangbao H., Bingfeng Y., Zhi C., Tiantian L., Min L. "Numerical investigation on the urban heat island in an entire city with an urban porous media model". *Atmospheric Environment*, 47, 509-518, 2012.

[20] Zhuangming Z., Junmin L., Wenjing Z., Jing Y., Shibin Q., Min X. "A numerical study of island wakes in the Xisha Archipelago associated with mesoscale eddies in the spring". *Ocean Modelling*, 139, 101406, 2019.

[21] Lidia L. V., Hiroyuki K. "Study on the urban heat island in Sofia City: Numerical simulations with potential natural vegetation and present land use data". *Sustainable Cities and Society*, 40, 110–125, 2018.

[22] Van Q. D., Hiroyuki K., Truong M., Nguyenb C. "Roles of past, present, and future land use and anthropogenic heat release changes on urban heat island effects in Hanoi, Vietnam: Numerical experiments with a regional climate model". *Sustainable Cities and Society*, 47, 101479, 2019.

[23] Lee, H. S., Trihamdani, A. R., Kubota, T., Iizuka, S., & Phuong, T. T. T. "Impacts of land use changes from the Hanoi Master Plan 2030 on urban heat islands: Part 2. Influence of global warming". *Sustainable Cities and Society*, https://doi.org/10.1016/j.scs.2017.02.015, 31, 95–108, 2017.

[24] Kubota, T., Lee, H. S., Trihamdani, A. R., Phuong, T. T. T., Tanaka, T., & Matsuo, K. "Impacts of land use changes from the Hanoi Master Plan 2030 on urban heat islands: Part 1. Cooling effects of proposed green strategies". *Sustainable Cities and Society*, https://doi.org/10.1016/j.scs.2017.04.001., 32, 295–317, 2017.

[25] Kusaka, H., Kimura, F., Hirakuchi, H., & Mizutori, M. "The effects of land-use alteration on the sea breeze and daytime heat island in the Tokyo metropolitan area". *Journal of the Meteorological Society of Japan*, 78(4), 405–420. https://doi.org/10. 2151/jmsj1965.78.4_405., 2000.

[26] Henk K. V., Weeratunge M., An Introduction to Computational Fluid Dynamics: The Finite Volume Method. Pearson Education Limited. ISBN 9780131274983, 2007.

[27] Blocken B., Carmeliet, J., Stathopoulos, T., "CFD evaluation of wind speed conditions in passages between parallel buildings—effect of wall-function roughness modifications for the atmospheric boundary layer flow", Journal of Wind Engineering and Industrial Aerodynamics 95, 941–962, 2007.

[28] ANSYS CFX Solver Theory Guide, 2011.

[29] CFX Limited,Waterloo, Ontario, Canada, CFX-Task flow Theory Documentation, Section 4.1.2, Version 2.12, 2002.

[30] Menter, F. R. Two-equation eddy-viscosity turbulence models for engineering applications. AIAA J. 32(8), 1598–1605, 1994.

[31] Versteeg, H. K., Malalasekera, W., An introduction to Computational Fluid Dynamics: The Finite Volume Method. Pearson Education, 2007.

[32]Launder, B. E., Spalding, D. B., "The numerical computation of turbulent flows". *Computer Methods in Applied Mechanics and Engineering*, 3, (2): 269–289., March 1974.

[33] Can O. F.. "Fluid Flow and Heat Transfer in a Channel with Noncircular Obstacles", *Arabian Journal for Science and Engineering,* 41:4291–4302, 2016.

[34] Surjamanto W., Inge M. S., Mardiyati Y., Andoni H., Rizky A. A., Steven S., Dixon T., Tunçbilek E., Arıcı M., Rahmah N., Tedja S. "Effect of different building façade systems on thermal comfort and urban heat island phenomenon: An experimental analysis". *Building and Environment*, 217, 109063, 2022.

[35] Meng, F., Guo, J., Ren, G., Zhang, L., Zhang, R., "Impact of urban heat island on the variation of heating loads in residential and office buildings in Tianjin". *Energy and Buildings*.,https://doi.org/10.1016/j.enbuild.2020.110357, 226, 110357, 2020.

[36] Boccalatte, A., Fossa, M., Gaillard, L., Menezo, C., "Microclimate and urban morphology effects on building energy demand in different European cities". *Energy and Buildings*.https://doi.org/10.1016/j.enbuild.2020.110129, 224, 2020.

[37] Gunawardena, K., Steemers, K., "Adaptive comfort assessments in urban neighbourhoods: simulations of a residential case study from London". *Energy and Buildings*. https://doi.org/10.1016/j.enbuild.2019.07.039., 202, 2019

[38] Guattari, C., Evangelisti, L., Balaras, C.A. "On the assessment of urban heat island phenomenon and its effects on building energy performance: a case study of Rome (Italy) ". *Energy and Buildings*. https://doi.org/10.1016/j. enbuild.2017.10.050., 158, 605–615, 2018.

[39] Cengel Y., Cimbala J. M., Fluid Mechanics fundamentals and applications, McGraw-Hill Series in Mechanical Engineering, ISBN 0–07–247236–7, 564-576, 2006

[40] Cung H. Nguyen, Dinh T. Nguyen, John S. Owen, David M. H. "Wind tunnel measurements of the aerodynamic characteristics of a 3:2 rectangular cylinder including non-Gaussian and non-stationary features". *Journal of Wind Engineering & Industrial Aerodynamics*, 220, 104826, 2022.

[41] Mannini, C., Massai, T., Marra, A.M., "Unsteady galloping of a rectangular cylinder in turbulent flow". *Journal of Wind Engineering and Industrial Aerodynamics.* 173, 210–226, 2018.

[42] Selimli S, "Numerical investigation of the effect of surface geometry on bullet aerodynamic behaviours", Journal of Polytechnic, 24(1): 299- 304, 2021.

[43] Kaya, M., "Investigation of Velocity and Pressure Distribution at Surrounding Airfoil Structure By Computatıonal Fluıd Dynamıcs Method", EÜFBED- Fen Bilimleri Enstitüsü Dergisi 4 (1), 59-69, 2011.

[44] Tekkalmaz, M. (2013). "Sinusoidal Duvarlı Kapalı Dikdörtgen Kutularda Hava Akışı ve Doğal Taşınım ile Isı Geçişi", Isı Bilimi ve Tekniği Dergisi, 33 (1), 21-31, 2013.